Desalination and Water Treatment
www.deswater.com

doi:10.5004/dwt.2019.23164

137 (2019) 88–100
January

Equilibrium and kinetic studies on the process of removing chromium(VI) from solutions using HDTMA-modified halloysite

Krystyna Kurdziel[a,*], Marta Raczyńska-Żak[a], Lidia Dąbek[b]

[a]*Institute of Chemistry, Jan Kochanowski University, Świętokrzyska 15G, 25-406 Kielce, Poland,*
emails: krystyna.kurdziel@ujk.edu.pl (K. Kurdziel), m.raczynska.zak@gmail.com (M. Raczyńska-Żak)
[b]*Faculty of Environmental, Geomatic and Energy Engineering, Kielce University of Technology,*
al. Tysiąclecia Państwa Polskiego 7, 25-314 Kielce, Poland, email: lidiadabek@wp.pl

Received 17 February 2018; Accepted 15 September 2018

ABSTRACT

The possibilities of applying halloysite in removing toxic anions of chromium(VI) compounds from aqueous solutions were examined in this work. Natural halloysite obtained from the Dunino mine in Poland was modified with intralayer cation exchange for hexadecyltrimethylammonium cations. The influence of the modification on halloysite structure was described with the use of a scanning electron microscope (SEM) together with surface analysis using energy dispersive X-ray spectroscopy (EDS/EDX), texture characteristics on the basis of N_2 adsorption–desorption analysis, as well as Fourier-transform infrared spectroscopy (FTIR). Chromium(VI) equilibrium isotherms were determined in the following temperature ranges: 293K, 303, 313K, and 323K. The experimental isotherms were analyzed on the basis of the Freundlich equation, as well as Langmuir, Temkin and Dubinin-Raduskevich models. It was observed that the Langmuir isotherm perfectly described the experimental data with respect to adsorption equilibrium. Process thermodynamics was characterized together in determining isothermal adsorption heat. Chromium(VI) adsorption kinetics was discussed based on the following models: pseudo-first order, pseudo-second order, Elovich, intraparticle diffusion, and the film diffusion model. Pseudo-second-order reaction rate constants determined at four various temperature values were applied in setting activation energy. Process effectiveness, that is, removing toxic chromium(VI) from the solution with the modified halloysite, is high, reaching 80%.

Keywords: Organoclays; Models adsorption; Chromium(VI) removal; Kinetic adsorption; HDTMA; Halloysite

1. Introduction

Elimination of pollution from sewage, especially from industrial effluents, is still an important and up-to-date problem. Chromium compounds, and in particular toxic Cr(VI) anions, are among the more hazardous pollutants penetrating into the environment. The sources of environmental pollution with chromium(VI) compounds include sewage from leather industry, galvanising plants, and dye and pigment production [1–3]. Among the methods currently used to treat sewage containing chromium compounds, the following should be mentioned: membrane filtration, ion exchange, extraction, electrochemical methods, and adsorption [1–12]. Method selection depends on physicochemical properties of sewage subject to treatment, formal requirements set for treated sewage, and costs. Whereas, it should be noted that it is not always necessary to completely eliminate certain pollutant, it is enough to reduce its concentration to an acceptable level.

Among numerous sorbents used to remove chromium compounds, more and more attention is given to mineral sorbents due to their availability, effectiveness, and relatively

---

* Corresponding author.

1944-3994/1944-3986

low costs involved in preparing them for use [2]. Among the minerals, which may be employed to eliminate toxic anions of chromium(VI), the following have been examined: kaolinite [13,14], chabasite [15], bentonite [16], clinoptiolite [17],and montmorillonite [14], although efforts are still made to find new sorbents. In the group of mineral sorbents, halloysite is more widely used.

The research on possible applications of clay minerals, for example, halloysite among others, is intense due to rich resources worldwide, their low cost, as well as several advantageous physiochemical properties, for example, the easiness to obtain, chemical and mechanical strength, and thermal stability. Their ecological neutrality cannot be neglected either.

Halloysite has found its application in various industrial branches. Due to its rheological properties, halloysite is utilized in producing ceramics and pottery and ceramic tiles, as well as in the paper industry. In the paint industry, it is used as paint, varnish, and ink thickener. It can be applied in order to improve the mechanical properties of cements and polymers [18,19].

In terms of chemical properties, halloysite is aluminosilicate, in which silicon-oxygen tetrahedrons $[SiO_4]^{4-}$ together with silicon-oxygen-hydroxyl octahedrons $[AlO_3(OH)_3]^{6-}$ form double-layer packs (1:1). Because of its crystal structure, the presence of natural nanotubes, huge porosity, and ion exchange capacity, halloysite can potentially be utilized in environmental protection as a sorptive agent to various chemical contaminants. Halloysite adsorbs cation forms due to its negative surface charge. A significantly wider application potential of this mineral is to be found on diverse chemical modification methods of the sorptive surface, among others, ion exchange with organic cations. Definitely wider range of application for this mineral is guaranteed by various chemical methods of the sorptive surface modification, which include ion exchange with organic cations. This sort of mineral modification dates back to the 1930s, in particular the study by Gieseking [20] concerning the ion exchange in minerals carried out using amines of different order. The history of derivation and the use of organominerals are discussed in detail in the studies by Betega de Paiva and Lee [21,22]. Since the mid-1980s, particular research interest has been aimed at using surfactants to modify minerals, in particular, including cationic surface-active agents, that is, quaternary long-chain ammonium salts. Hexadecyltrimethylammonium (HDTMA) bromide or chloride [23] are the most commonly used agents. The $HDTMA^+$ cation has positive charge located on the nitrogen atom of the amine group and hydrophobic alkyl chain. The surface of minerals intercalated with $HDTMA^+$ is stable at extreme values of pH and ionic strength, and in organic solvents [23]. It is also important to note that this amine is an easily available and the cheapest compound in this group of surfactants. Mineral modification with $HDTMA^+$ may take place in two ways, depending on the concentration of surface-active agent in a solution. When the HDTMA equilibrium concentration is below its critical micelle concentration (CMC), interlayer cations of the mineral are replaced by sorbent cations – $HDTMA^+$. Positively charged surfactant "head" interacts with negative mineral surface, covering the surface with a monolayer. The adsorbent modified in this way is capable of sorption from solutions of poorly polar and nonpolar molecules, for example, from organic compounds.

At higher concentrations, the intercalated $HDTMA^+$ cations from monolayer make additional bonding with others (not bound with the surface) by hydrophobic action of alkyl chains ("tails"), thus forming a bilayer or ad-micelles [23–26]. As a result of this arrangement of $HDTMA^+$ ions, the adsorbent surface charge turns into positive, and thus the originally cation exchange mineral changes its affinity toward adsorption from negative ion solutions.

Our objective in this work is to examine the possibilities of applying HDTMA-modified halloysite in removing anionic chromium(VI) compounds from aqueous solutions.

Static method measurements were implemented to complete the above-stated objective of the work. The relationship between chromium(VI) adsorption and solution pH was analyzed. Process kinetics was studied on the basis of pseudo-first as well as pseudo-second-order models, the Elovich model, the intraparticle diffusion model and the film diffusion.

Isotherm interpretation was based on the selected two-parameter adsorption models. They were subsequently used in order to determine thermodynamic parameters of the studied process. Chromium(VI) adsorption study was preceded by determining the adsorptive capacity of natural halloysite against HDTMA. In addition, surface parameters of the modified mineral were described.

2. Experimental

2.1. Preparation of modified form of halloysite (hal-HDTMA)

Halloysite (Dunino mine in Poland) with a particle diameter of 0.12–0.25 mm was rinsed with distilled water several times. 100 g sample of the mineral was added to 1 dm^3 2 M of the NaCl solution and shaken for 24 h. The sodium form of halloysite was thus obtained. It was subsequently rinsed with distilled water to moment of the negative test for chlorides with $AgNO_3$ in the equilibrium aqueous phases. The mineral was then filtered off and dried in open air.

In the subsequent modification stage, the obtained halloysite form was added to a solution containing 2.5 g of hexadecyltrimethylammonium bromide (HDTMA) in 1 dm^3 of water. The mixture was gently shaken for 24 h. A modified form of halloysite was obtained in this manner (hal-HDTMA), which was filtered off and dried in open air.

2.2. Characterization of adsorbent

The studies on adsorptive halloysite capability in relation to hexadecyltrimethylammonium ($HDTMA^+$) cation were based on marking adsorbate concentration in the solution before and after the interaction with halloysite by applying quantitative analysis of the concentration with respect to complete organic carbon in the solution. Output concentration values of HDTMA were in the range of 0.8–1,250 mg/dm^3. Solution volumes in all measurements equaled 15 cm^3, while the weight of the sodium halloysite form (obtained according to the procedure described earlier) was 1 g. The solutions were shaken at a constant rate of 120 rpm using the thermostat at a temperature of 293K. HDTMA concentration in the solution, after contact with halloysite, was marked with organic carbon analysis using the STAR TOC Auto Benchtop analyzer, which is equipped with two NDIR detectors by TOC System Inc.

Raw halloysite and HDTMA-modified halloysite were described with SEM, together with surface analysis with the use of EDS/EDX methods. The characteristics of the natural, as well as HDTMA-modified halloysite, was conducted on the basis of adsorption/desorption isotherms of nitrogen pairs at a temperature of 77K, which were recorded with an ASAP 2020 adsorptive analyzer by Micrometrics (Norcross, GA, USA). Prior to measurements, adsorbent samples were degassed at 473K.

2.3. Adsorption experiments

The adsorptive properties of the halloysite modified according to the procedure described earlier, that is, hal-HDTMA, were studied using $K_2Cr_2O_7$ (Polish Chemical Reagents, p.f.a.) as a source of toxic chromium(VI).

Initially, the relationship between chromium(VI) adsorption and the adsorbate pH solution was analyzed. For this reason, a series of chromium(VI) solutions with constant concentration, that is, 210 mg/dm^3, and various reactions were prepared. They were regulated with 1 M HCl or 1 M NaOH. A quantity of 1 g sample of the hal-HDTMA halloysite was poured with 15 cm^3 of the prepared solutions. Chromium(VI) concentration was marked after 24 h.

In the conducted adsorption measurements, initial and equilibrium concentration values of Cr(VI) were spectrophotometry-marked with the use of diphenylcarbazide [27] and a UV–VIS–NIR UV-3600 Shimadzu spectrophotometer. Absorbance was measured at a wavelength of 545 nm.

In the study of process kinetics, 1 g weighted amounts of hal-HDTMA were in contact with a 15 cm^3 chromium(VI) solution at a concentration of 175 mg/dm^3 at different time values, that is, between 5 and 360 min.

Adsorption isotherms were determined through marking the chromium(VI) concentration change in solutions with the concentration of Cr(VI) from 15 to 235 mg/dm^3, in contact with hal-HDTMA for 4 h (1 g weighted amounts of hal-HDTMA were poured with 15 cm^3 of the $K_2Cr_2O_7$ solution).

Chromium(VI) concentration adsorbed on hal-HDTMA was calculated according to the following formula:

$$q_e = \frac{\left(C_0 - C_e\right)V}{m} \tag{1}$$

where C_0 and C_e (mg/dm^3) are the initial and equilibrium chromium(VI) concentrations of solutions, V (dm^3) is the volume of the solution, and m (g) is the dosage of halloysite samples.

Process efficiency (E) of removing chromium(VI) from the solution was calculated according to the formula below:

$$E = \frac{C_0 - C_e}{C_0} \times 100\% \tag{2}$$

The pH values of the equilibrium solutions were controlled using a combined glass electrode (EPS-1) connected to the pH-meter (Elmetron pH-meter C401).

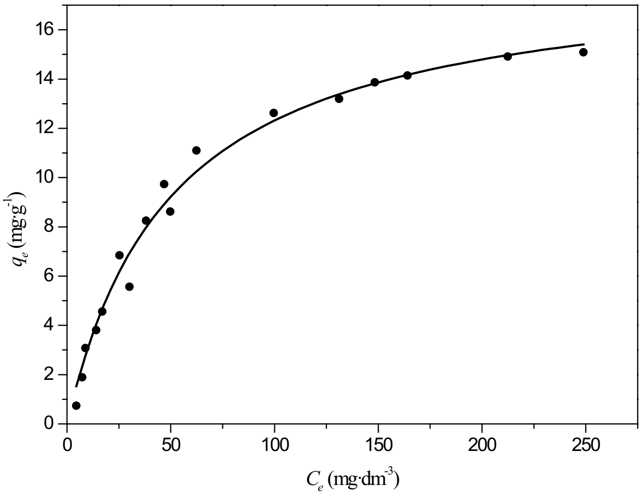

Fig. 1. The adsorption isotherm of HDTMA$^+$ on the halloysite at 293K.

3. Results and discussion

3.1. Characterization of adsorbent (hal-HDTMA)

3.1.1. HDTMA adsorption on halloysite

Organic carbon contents in the solution showed that as a result of sorption on 1 g of halloysite, a maximum of 12.02 mg of carbon disappeared from a solution. This is in parallel with the quantity of 15 mg of HDTMA$^+$ cations (0.0527 mmol/g and 19.21 mg/g HDTMA, respectively). The HDTMA$^+$ adsorption isotherm on raw halloysite is illustrated in Fig. 1.

It has been observed that the experimental data is described best by the Langmuir model. Equilibrium constant K_L is 0.02218 dm^3/mg (correlation coefficient R^2 = 0.9857).

The concentration, at which maximum coverage of halloysite surface with HDTMA (C_0 = 1,240 mg/dm^3) has been reached, is higher than the critical micellar concentration of this surfactant (CMC = 0.94 mmol/dm^3 = 342.6 mg/dm^3). Then, it should be concluded that the HDTMA$^+$ cations cover the mineral surface in bilayers or in a hemi-micellar way. Therefore, modified halloysite should show adsorption affinity toward chromium(VI) anions.

3.1.2. Halloysite morphology

SEM images (Figs. 2(a)–(c)) of raw halloysite samples illustrate a nonhomogeneous plate-tube layer structure of the mineral, as well as the presence of aggregates (clusters of several fine particles). The average size of halloysite particles was ca. 0.2 μm, and the longest observed nanotubes were 1 μm in length and ca. 0.1 μm in diameter. On the basis of SEM images (Figs. 2(d)–(f)) of the modified halloysite, it was determined that the mineral structure did not change. Surfactant hexadecyltrimethylammonium (HDTMA$^+$) cations were attached to the clay mineral surface without any deformation of the main halloysite structure.

3.1.3. Texture

Adsorption/desorption isotherms of nitrogen pairs on raw halloysite, as well hal-HDMTA, are illustrated in Fig. 3.

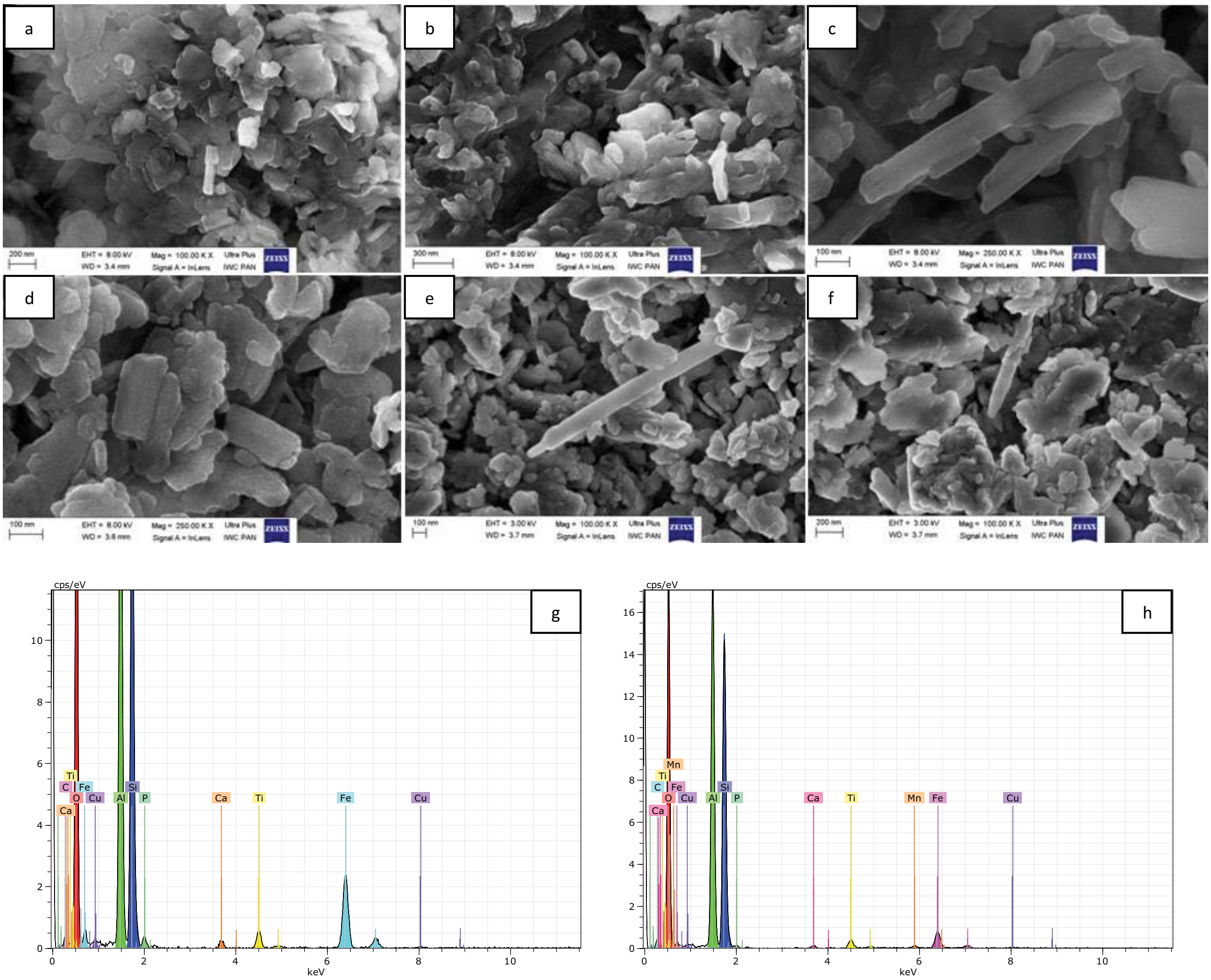

Fig. 2. SEM images and EDX spectra of raw (a, b, c, g) and HDTMA-modified halloysite (d, e, f, h).

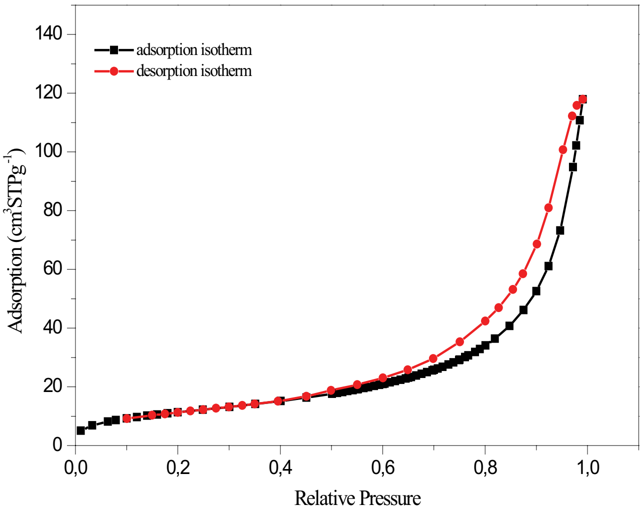

Fig. 3. Nitrogen adsorption-desorption isotherms of halloysite-modified HDTMA.

The classification of isotherms, the observed hysteresis loops and the resultant interpretation was conducted applying IUPAC guidelines [28].

Initial quality-related information on volumetric as well as surface properties of pores in an adsorbent is provided with the adsorption/desorption isotherm course of nitrogen pairs.

The obtained adsorption/desorption curves (Fig. 3) have IV type isotherm features, according to IUPAC guidelines. Initially, the curves have a smooth course at low and medium relative pressure values. Low adsorption in this range corresponds to filling nitrogen pores in a monolayer. Subsequently, beginning with p/p_0 equal to 0.8, adsorption increases sharply to reach the borderline value.

Such course of the discussed isotherms indicates the presence of mesopores, the structure of raw halloysite, as well as hal-HDTMA (adsorption at low pressure values would indicate the presence of micropores).

Another feature of the isotherm of IV type is the occurrence of the hysteresis loop [28].

The presence of the aforementioned loops is connected with a varied course (depending on relative pressure values)

Table 1
Structural parameters of raw and HDTMA-modified halloysite (hal-HDTMA)

Materials	S_{BET} [m^2/g]	V_t [cm^3/g]	D [nm]
Halloysite	46	0.1925	16.74
hal-HDTMA	40	0.1658	16.58

of filling and releasing pores with nitrogen molecules. The shape of the hysteresis curve facilitates drawing a conclusion about the character and the shape of pores present in the adsorbent. The course of the analyzed loops allows for qualifying them to type H3, corresponding to the material with cavity pores, often described as "bottled."

Qualitatively, the obtained adsorption/desorption isotherms of nitrogen pairs were interpreted by calculating the surface and volumetric parameters of the examined adsorbents, that is, specific surface area, volume, and pore diameter. Specific surface area (S_{BET}) was determined in the range of relative pressure values p/p_0 from 0.05 to 0.2 on the basis of the Brunauer–Emett–Teller method [29]. Single nitrogen molecule area, that is, 0.162 nm^2, in the monolayer was taken into consideration with respect to the calculations. The total porous volume (V_t), which is the volumetric sum of micropores and mesopores (V_{me}), was determined from a single point nitrogen adsorption isotherm relating to relative pressure, that is, p/p_0 = 0.99. The pore diameter (D) was marked using the following formula: $D = 4\ V_t/S_{BET}$. The adsorbent structure parameters are shown in Table 1. The surface area (S_{BET}) of the studied raw halloysite is 46 m^2/g, while for hal-HDTMA (modified with a surface-active agent), it is a bit smaller, that is, 42 m^2/g. The determined texture parameters indicate that the studied adsorption materials do not have micropores. However, marking micropores is not always possible. This is owing to the fact that they can be taken by nonlattice ions, which hinder the penetration of nitrogen molecules. Mesopores are definitely dominant in the structure of both raw halloysite as well as hal-HDTMA.

Data compilation in Table 1 shows that surface modification is followed by a slight diminishing of textural parameters. This change results from partial blocking of the halloysite porous surface by cations of the adsorbed surfactant, that is, HDTMA$^+$ ions.

3.1.4. Infrared spectra

Absorption bands are grouped in two areas of the infrared spectra of natural halloysite. The first is in the range of 3,700–340 cm^{-1}, whereas the second 1,700–400 cm^{-1}. In the most frequent occurrence area, there are two separated medium intensity bands at 3,696 and 3,623 cm^{-1}, corresponding to expanding vibrations of surface hydroxyl groups: Si–Si–OH and Al–Al–OH. In the next adsorption area, a wide, diffused, and weak intensity band, with its center at 1,632 cm^{-1}, is assigned to water bending modes within the clay interlayer.

At the frequency occurrence range of 1,200–600 cm^{-1}, there are vibrations of skeletal bonds in aluminosilicate polyhedral. Absorption connected with stretching Si–O vibrations is represented on a sharp band by a high-intensity pack of 1,038 cm^{-1}. The deforming vibration band, Al_2O–H, occurs at 914 cm^{-1}. A band at 538 cm^{-1} may be observed as well, which corresponds to the vibrations of Al–O–Al, together with the vibration band of Si–O–Si at 470 cm^{-1} [30].

Apart from the already described bands for the natural halloysite, there are two new bands visible, stemming from methylene group vibrations of the alkyl chain surfactant present in the structure of the modified mineral. They are connected with both symmetrical (ν_s) and asymmetrical (ν_{as}) vibrations of C–H bonds. These bands are present at 2,848 and 2,920 cm^{-1}, respectively.

As regards hal-HDTMA, the bands stemming from the vibrations surfactant molecule bonds can be observed, apart from bands typical of raw halloysite, that is, at 2,800–3,000, 1,350–1,550, 2,800–3,000, and 1,350–1,550 cm^{-1} (with the center at 1,475 cm^{-1}). The last faintly-marked spectrum on the band, at 1,475 cm^{-1}, is assigned to the bending vibration of C–H in methylene group.

The most typical and intense surfactant molecule bands are bonded with symmetrical (υ_s) and asymmetrical (υ_{as}) C–H bond vibrations in the methylene groups of the alkyl chain; they are present at 2,848 and 2,920 cm^{-1}, respectively. Band positioning is altered together with the increase of HDTMA contents in the halloysite. Namely, these bands shift toward higher frequency values, that is, up to 2,856 and 2,923 cm^{-1}, respectively. Such a change is connected with the large sensitivity of frequency values (as regards vibrations stretching C–H in the alkyl chain) to conformational changes of the long alkyl chain from the unordered, synclinal (*gauche*) to the ordered (*trans*) [31,32].

The antisymmetric CH_2 stretching mode is more sensitive to the conformational ordering than the symmetric stretching mode [30,33,34]. Shifting these bands indicates an increasing *trans* conformer impact together with an increase of HDTMA contents in the halloysite structure. When surfactant concentration is low (below the critical micellization level) in the interlayer halloysite surface, HDTMA$^+$ cations are positioned in the monolayer with the *gauche* conformation (unordered). At higher concentration levels of HDTMA, there is an increase in the intrachain van der Waals interaction, and a double layer is generated [35], which results in ordering the chain into the *trans* form. At high amounts adsorbed HDTMA$^+$ ions (e.g. >100% CEC) hydrophobic HDTMA$^+$ tails have a tendency to adopt a micelle-like system [36,37]. Both bilayer and micellar adsorbent surface coverage creates the possibility of adsorbing anion forms.

3.2. Chromium(VI) removal studies

3.2.1. Effect of pH on chromium(VI) adsorption

As a result of the conducted measurements on the relationship of chromium(VI) adsorption on the HDTMA modified halloysite and the solution pH, it was determined that in an acidic environment with pH = 2.1–6, the acidic value was the highest and constant, that is, 1.53 mg/g. In the solutions with higher pH values, there was a rapid adsorption decrease; at pH = 8.65, the decrease of hal-HDTMA adsorptive capacity was up to 43% (to 0.66 mg/dm^3). Further equilibrium and kinetic measurements of the adsorption process were conducted in an acidic environment at pH = 4.5.

In acidic solutions, chromium(VI) anions occur in the form of $Cr_2O_7^{2-}$ and $HCrO_4^-$ [38]. Concentration of the two forms of chromium(VI) in the state of equilibrium depends on the total chromium concentration in the solution. It needs to be assumed that chromium(VI) adsorption on the modified halloysite with $HDTMA^+$ cations takes place by the interaction of both anions $Cr_2O_7^{2-}$, as well as $HCrO_4^-$ with a positive charge of the ammonium part of the molecule, that is, the so-called "surfactant head."

3.2.2. Adsorption kinetics

Adsorption measurements, depending on the contact time of the hal-HDTMA phase constant with chromium(VI) anions, were used to determine the kinetic parameters and the rate of the process.

Kinetic measurements were conducted at four temperature values: 293K, 303K, 313K, and 323K. Fig. 4 illustrates the changes in mass of the absorbed chromium(VI) into 1 g hal-HDTMA, occurring together with the process time change (q_t vs t).

As stems from the diagrams, chromium(VI) adsorption takes place at two stages. The initial stage of rapid adsorption occurs for the first 60 min of the process. This is followed by a stage of slow process toward the equilibrium state in approximately 180 min.

The kinetics with respect to the process of removing Cr(VI) from the solution using HDTMA-modified halloysite was analyzed on the basis of the Elovich model [39,40], the pseudo-first-order model [41], the pseudo-second-order model [42–44], as well as the Weber–Morris intraparticle diffusion model [45,46], and the film diffusion model [47,48].

The kinetic Elovich model considers the participation of the chemisorption process on the adsorbent heterogeneous surface [39].

It is described with the equation as follows:

$$q_t = \frac{1}{\beta}\ln(\alpha \times \beta) + \frac{1}{\beta}\ln t \qquad (3)$$

where α is an initial adsorption rate (mg/g min), and β is similar to the surface coverage degree, as well as activation energy for chemisorption (mg/g).

The relationship q_t with ln(t) has a linear course with slope angle $1/\beta$ and interception with the y-axis $\frac{1}{\beta}\ln(\alpha \times \beta)$.

Kinetic measurement α and β parameter values calculated at temperature values 293K, 302K, 313K, and 323K are shown in Table 2. The values of correlation coefficients R^2 for the linear relationship take values from 0.88 to 0.97. The initial rates of chemical adsorption α or surface coverage determined with the β coefficient do not correspond to experimental data. Thus, the Elovich kinetics model is not appropriate to interpret the studied chromium(VI) adsorption processes on the modified halloysite mineral.

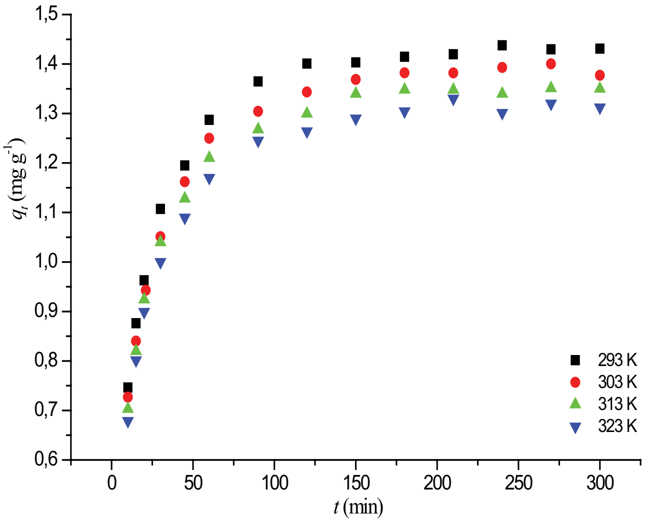

Fig. 4. Effect of contact time on the removal of chromium by hal-HDTMA at 293K, 303K, 313K, and 323K.

Table 2
Kinetic parameters for adsorption chromium(VI) onto HDTMA-modified halloysite

Kinetic model	Parameters	T (K)			
		293	303	313	323
Pseudo-second order	$q_{e,\exp}$ (mg/g)	1.52	1.45	1.36	1.32
	$q_{e,\mathrm{cal}}$ (mg/g)	1.52	1.47	1.41	1.36
	k_2 (g/mg min)	0.0569	0.0586	0.0670	0.0726
	R^2	0.9988	0.9999	0.9992	0.9985
Elovich	α (mg/g min)	0.4052	0.5325	1.2122	1.0770
	β (mg/g)	3.718	4.136	5.097	7.299
	R^2	0.9724	0.9634	0.9880	0.8946
Interpractice diffusion	Intercept	1.1319	1.0796	0.904	0.8668
	k_t (mg/g min$^{0.5}$)	0.0246	0.0229	0.0336	0.0330
	R^2	0.9190	0.9855	0.9926	0.9921
Liquid film diffusion	Intercept	–0.6471	–0.8323	–0.3981	–1.1534
	k_{fd} (min^{-1})	0.0141	0.0137	0.0302	0.0182
	R^2	0.9248	0.9276	0.9287	0.9622

The kinetics of adsorption reaction occurring according to the pseudo-first-order model is illustrated in the equation as follows [41]:

$$\frac{dq_t}{dt} = k_1\left(q_e - q_t\right) \tag{4}$$

During data analysis, the linear form, obtained from Eq. (2) as a result of algebraic transformations, is the most frequently used as follows:

$$\ln\left(q_e - q_t\right) = \ln q_e - k_1 \times t \tag{5}$$

The adsorption process, progressing in time according to the pseudo-second-order mechanism [42], is described in the following equation:

$$\frac{dq_t}{dt} = k_2\left(q_e - q_t\right)^2 \tag{6}$$

which was popularized in the linear form by Ho [43,44] as

$$\frac{t}{q_t} = \frac{1}{k_2 q_t^2} + \frac{t}{q_e} \tag{7}$$

where k_1 – the pseudo-first-order equilibrium adsorption rate constant (min^{-1}); k_2 – the pseudo-second-order equilibrium adsorption rate constant (g/mg min); q_t and q_e – the solid phase chromium(VI) concentrations at time (t) and equilibrium (mg/g), respectively.

The relationship of ln(q_e – q_t) versus t [Eq. (5)], which describes the pseudo-first-order kinetics, is not straight linear at four temperature levels. They are deviated from linearity, particularly in the proximity of the equilibrium state; for this reason, correlation coefficients R^2 are unsatisfactory. It can be deduced that the pseudo-first-order kinetic model is not appropriate to describe the course of the discussed adsorption process.

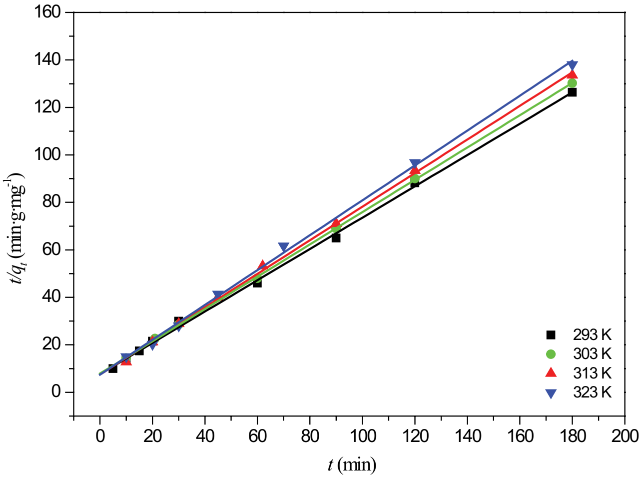

Fig. 5. The pseudo-second-order kinetic for the adsorption of chromium onto the halloysite-HDTMA at different temperatures.

Definitely, better matching of experimental data was obtained for the pseudo-second-order kinetic model. Relationship diagrams (7) are linear (Fig. 5), whereas correlation coefficients R^2 are approximately 0.999 (Table 2). In addition, the calculated values of sorptive volumes q_e as regards chromium(VI) in the case of every temperature range correspond to experimental values. The aforementioned facts confirm the correctness of describing the kinetics of the studies chromium(VI) adsorption processes on the modified halloysite with the pseudo-second-order model. The determined adsorption process rate constants k_2 at 293K, 303K, 313K, and 323K are compiled in Table 2.

A comparison of the data presented in Table 2 shows that the reaction rate constant k_2 increases together with a temperature increase, indicating that adsorption occurs faster at higher temperature rates. However, the decreasing adsorption in the equilibrium state (q_e) (both the q_e calculated with the kinetic equation and the experimental equation) indicates the exothermic character of the discussed chromium(VI) adsorption processes.

Further discussions concerned the impact of diffusion on adsorption rate. For this reason, the kinetics of chromium(VI) adsorption were analyzed on hal-HDTMA on the basis of the intraparticle diffusion model (IDM), the Weber-Morris model [45,46], as well as the liquid film diffusion model [47,48].

The first of the models is described with in following equation [45,46]:

$$q_t = k_{\text{in}} \times t^{0.5} + C \tag{8}$$

whereas the second is connected with the transport of the solute molecules from the liquid phase up to the solid phase [47] as follows:

$$\ln\left(1 - F\right) = -k_{\text{fd}} \times t \tag{9}$$

where F – the fractional attainment of equilibrium ($F = q_t/q_e$); k_{fd} – the adsorption rate constant

If the kinetics of the adsorption process are controlled with diffusion by a liquid film surrounding constant adsorbents, the relationship diagram ln(1–F) versus t ought to have zero interception.

In the course of the relationship of q_t and $t^{0.5}$ drawn in time until reaching the equilibrium state, two straight lines at different slopes can be distinguished, which confirms two stages of overall adsorption rate. The second of these straight lines, according to the Weber–Morris model, is connected with intraparticle diffusion.

For straight lines describing the aforementioned relationship at four temperature values, the correlation coefficient R^2 is relatively high, present in the range of 0.92–0.99 (Table 2). Intraparticle diffusion rate constants are in the following range: 0.0229–0.0336. However, straight lines do not have zero interception (figure not shown). The linearity of the second part of the diagram (q_t vs $t^{0.5}$), confirmed with relatively high values of correlation coefficients R^2, denotes the fact that intraparticle diffusion plays a major role in the chromium(VI) adsorption process on the modified halloysite. Nevertheless, this is not the determinant stage concerning the rate of the whole process. This is marked with interception points of the straight line with the y-axis being different from zero (Table 2).

According to the film diffusion model (FDM), a certain concentration gradient is generated in direct proximity to the adsorbate (at a minuscule solution area), which results from rapid adsorption. This adsorbate "loss" is compensated with the diffusion process, determined as the diffusion model through a tiny liquid layer surrounding the adsorbate molecule. The relationship equation (9) is linear (figure not shown), and the correlation coefficients R^2 is relatively high, that is, 0.92–0.96 (Table 2); however, the straight line does not cross the starting point of the y-axis. Such a situation is not in concordance with Eq. (9); thus, it can be assumed that "diffusion through film" is not a stage determining the adsorption process.

3.2.3. Activation energy

From the pseudo-second-order rate constants k_2 (Table 2), the activation energy E_a for adsorption chromium(VI) on the modified halloysite was determined.

The Arrhenius equation was utilized to calculate the activation energy, which is given as follows:

$$k_2 = A \times e^{-\frac{E_a}{RT}} \tag{10}$$

$$\ln k_2 = \ln A - \frac{E_a}{R} \times \frac{1}{T} \tag{11}$$

where E_a is activation energy, J/mol, R is the gas constant (8.31 J/mol K), and A is the Arrhenius constant.

The change of rate constant (k_2) was analyzed together with the temperature, based on the relationship diagrams ln k_2 versus $1/T$ [Eq. (11)]. This relationship diagram is illustrated in Fig. 6.

The value of activation energy with respect to the chromium(VI) adsorption process from an aqueous solution equals 7.603 kJ/mol, which proves the physical character of the process.

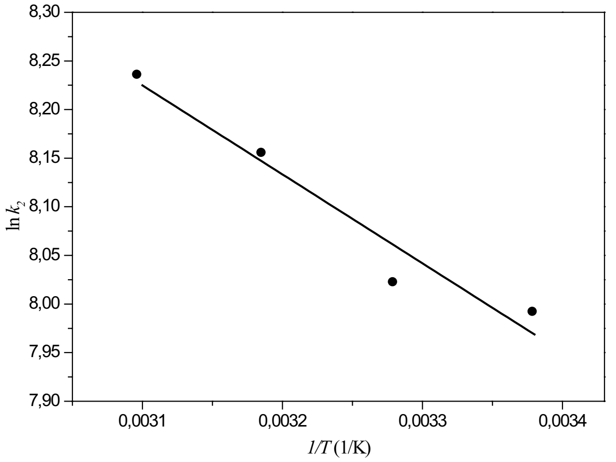

Fig. 6. Plot of ln k_2 versus $1/T$ for estimation of activation energy for the adsorption of chromium on hal-HDTMA.

3.2.4. Adsorption isotherms

Chromium(VI) adsorption isotherms from aqueous solutions on the modified halloysite (hal-HDTMA) were determined at: 293K, 303K, 313K, and 323K. Their course is illustrated in Fig. 7.

The preceding diagrams show that together with a temperature increase, adsorption decreases, which proves the exothermic character of the discussed process.

At the temperature of 293K, maximum sorptive capacity of chromium(VI) on hal-HDTMA is 1.55 mg/g. The sorptive capacity of other minerals modified with the same surface-active agent is highly diversified and, for example, in the case of kaolinite it is 0.68 mg/g [13], chabasite 2.6 mg/g [14], bentonite 19 mg/g [15], clinoptiolite 9.46 mg/g [16], and montmorillonite41.6 mg/g of this mineral [17]. The presented comparison shows that admittedly hal-HDTMA has less sorptive potential than the three-layer minerals, but it is by far higher than for a structurally analogical mineral – kaolinite.

Temkin [49], Dubinin-Raduskevich [50,51], Freundlich [52], and Langmuir [53] models were applied to interpret adsorption experimental isotherms.

The nonlinear regression model using Origin Microcal 10 (together with the Levenberg-Marquardt algorithm) was applied in order to assign an appropriate adsorption model and for the sake of calculating sorption parameters appropriate for each of the models.

Temkin isotherm parameters, Temkin adsorption potential (K_T), as well as the Temkin constant (B_T), were determined on the basis of the following equation [49]:

$$q_e = B_T \ln\left(K_T \times C_e\right) \tag{12}$$

and are compiled in Table 3.

The Temkin constant (B_T) is connected with adsorption heat ($\Delta Q = -\Delta H$), that is, $B_T = RT/\Delta Q$ (R – universal gas constant (kJ/mol K), T – temperature (K))

Enthalpy values (ΔH) determined on the basis of the aforementioned relationship, at four temperature values,

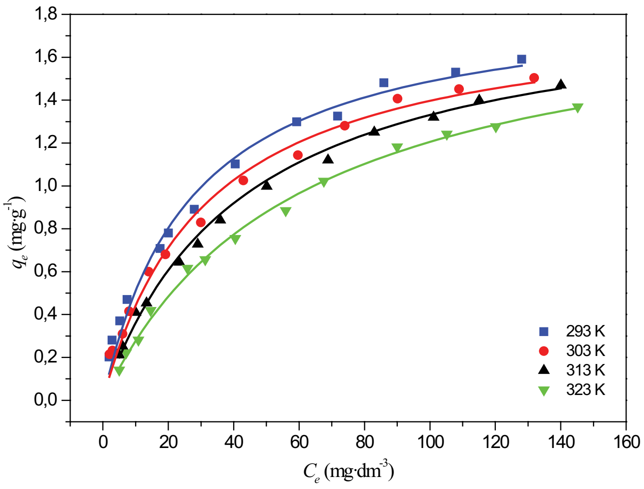

Fig. 7. The adsorption isotherms of chromium(VI) on the HDTMA-modified halloysite at different temperatures.

Table 3
Isotherm parameters for adsorption of chromium(VI) onto HDTMA-modified halloysite

Isotherm	Parameters	T (K)			
		293	303	313	323
Langmuir	K_L (l/mg)	0.03716	0.03173	0.02222	0.01687
	q_m (mg/g)	1.89	1.84	1.82	1.80
	R^2	0.9948	0.9938	0.9949	0.9938
Freundlich	K_F (mg/g) (L/mg)$^{1/n}$	0.2067	0.1723	0.1322	0.0966
	$1/n$	0.4807	0.4572	0.500	0.5444
	R^2	0.9901	0.9898	0.9816	0.9736
Temkin	K_T (L/g)	0.5192	0.3246	0.2511	0.1670
	B_T	0.3689	0.3985	0.4020	0.4229
	ΔH (kJ/mol)	–6.60	–6.32	–6.47	–6.35
	R^2	0.9748	0.9900	0.9855	0.9898
Dubinin-Radushkevich	q_m (mg/g)	4.90	5.13	5.20	6.18
	B (mmol^2/L^2)	5.04×10^{-9}	5.52×10^{-9}	5.91×10^{-9}	6.99×10^{-9}
	E (kJ/mol)	9.96	9.52	9.20	8.46
	R^2	0.9977	0.9913	0.9233	0.9881

take negative values characteristic of exothermal adsorption processes. They are ca. –6.5 kJ/mol (Table 3).

The Dubinin–Raduskievich isotherm [50,51] [Eq. (13)] describes adsorption in micropores, on homogeneous adsorbent surfaces.

$$q_e = q_m \times e^{-\beta\varepsilon^2} \tag{13}$$

Constant β is connected with sorption energy (E), which is defined as the free energy transfer of 1 mol of solute from infinity of the surface of the sorbent, and can be calculated using the relationship [54]

$$E = \frac{1}{\sqrt{2\beta}} \tag{14}$$

where q_m is theoretical saturation capacity, ε is Polanyi potential, which is equal to $RT(\ln(1 + 1/C_e)$, R (J/mol K) is the gas constant, and T (K) is the absolute temperature.

Parameter E enables differentiating between the physical and chemical adsorption. E values smaller than 8 kJ/mol are typical as regards physical sorption, whereas those in the 8–16 kJ/mol range represents the chemical adsorption [55]. In the studied chromium(VI) adsorption process, the E values change together with the temperature from 10.00 to 8.46 kJ/mol (see Table 3). However, no conclusions can be drawn with respect to adsorption type on the basis of the values mentioned earlier. Too large q_m values (Table 3) compared with experimental data explicitly indicate that this model cannot be applied to interpret the studied chromium(VI) sorption process.

The course of experimental data q_e versus C_e was additionally analyzed based on the Freundlich model [52]:

$$q_e = K_F \times C_e^{1/n} \tag{15}$$

where K_F is the adsorption volume constant [(mg/g)(dm^3/mg)$^{1/n}$] and 1/n is the empirical constant describing the heterogeneity of the adsorption process.

The calculated Freundlich constants (K_F), with the use of the Levenberg–Marquardt, as well as $1/n$, at four various temperature values, are presented in Table 3. Correlation coefficient R^2 is in the following range: 0.97–0.99. The Freundlich isotherm belongs to type L isotherms [56], and $1/n$ parameters are low, being in the range 0.49–0.65 (Table 3). The adsorption isotherm, plotted based on the Freundlich Eq. (15), does not match the obtained experimental isotherm (Fig. 8). Thus, the Freundlich model cannot be used to interpret the chromium(VI) adsorption on hal-HDTMA.

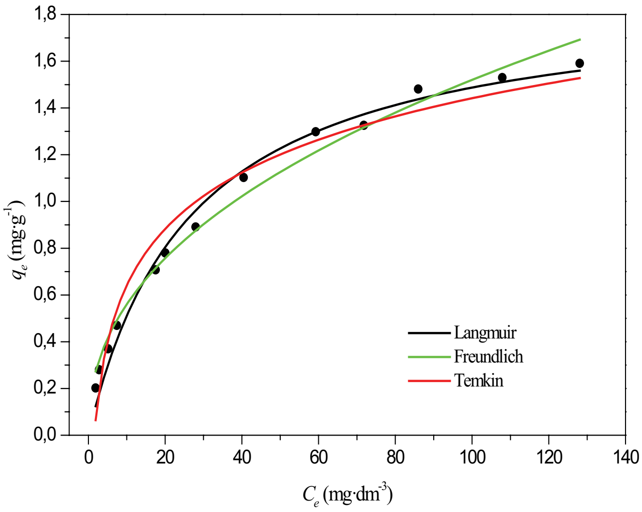

Fig. 8. Comparison of different isotherm models for the adsorption chromium(VI) onto hal-HDTMA at 293K.

Langmuir isotherm parameters q_m and K_L were calculated on the basis of the following equation describing this adsorption model:

$$q_e = q_m \times \frac{K_L C_e}{1 + K_L C_e} \tag{16}$$

where q_m is the maximum adsorption capacity corresponding to a complete monolayer coverage on the adsorbent surface (mg/g) and K_L is the Langmuir constant (dm^3/mg)

The results are compiled in Table 3. Adsorption equilibrium constants (K_L) become lower together with a temperature increase (a higher temperature facilitates desorption). This means that the discussed chromium(VI) adsorption process is exothermal.

High correlation coefficients R^2 (~0.99) for the Langmuir adsorption constants (K_L) determined at various temperatures (Table 3) are higher than in the case of the Freundlich model. Additionally, the concordance of the theoretical and experimental value of maximum adsorption capacity (q_m) indicates that the chromium(VI) adsorption process on the modified halloysite occurs according to the Langmuir model.

Fig. 8 illustrates an experimental chromium(VI) adsorption isotherm, determined at 293K, as well as the course of isotherms obtained on the basis of four analyzed theoretical models.

One can clearly notice that among the analyzed adsorption models, the course of the Langmuir isotherm [Eq. (16)] matches the experimental values (q_e vs C_e) to the largest degree. Moreover, this confirms the conclusion that the chromium(VI) adsorption on the modified halloysite (hal-HDTMA) displays the largest concordance level of the Langmuir model.

3.2.5. Adsorption thermodynamics

State functions: free energy (ΔG), enthalpy (ΔH), and entropy (ΔS), were determined in order to conduct thermodynamic characteristics of the studied chromium(VI) adsorption processes on the HDTMA-modified halloysite. The thermodynamic parameters were evaluated using the following equations:

$$\Delta G = -RT \ln K_L \tag{17}$$

$$\ln K_L = -\frac{\Delta H}{R} \times \frac{1}{T} + \frac{\Delta S}{R} \tag{18}$$

where K_L is the Langmuir constant, T is the absolute temperature (K), and R is the gas constant (8.314 J/mol K).

The parameters of straight-line relationship ln K_L versus 1/T determine the entropy, as well as enthalpy, values of the adsorption processes. A graphical image of the aforementioned relationship is shown in Fig. 9.

The determined values of thermodynamic parameters (ΔH, ΔS, ΔG) are given in Table 4. Negative values of the standard free energy (ΔG), at any temperature level of the process, are appropriate for spontaneous processes. The determined enthalpy value, ΔH = –21.29 kJ/mol, indicates the physical character of chromium(VI) processes on the modified halloysite adsorbent (for physical adsorption, ΔH ought to be <80 kJ/mol, while for chemical adsorption, it is in the range of 80–400 kJ/mol. Negative ΔH values confirm the exothermic character of the discussed processes.

An entropy decrease (ΔS = –9.02 J/mol) results from the fact that adsorbate particles lose their translatory and oscillatory freedom, which is a consequence of adsorption.

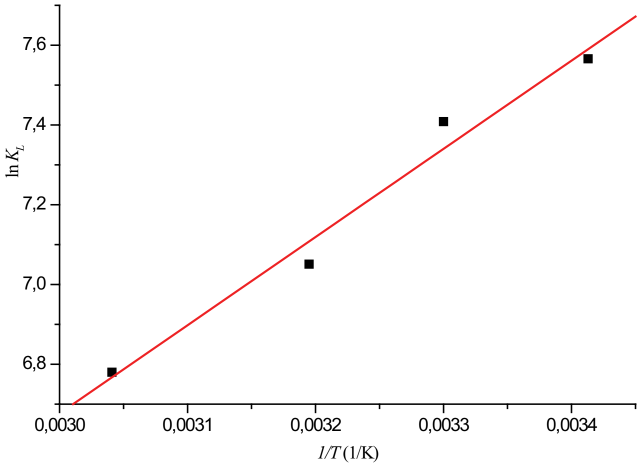

Fig. 9. Plot of ln K_L versus 1/T for the estimation of thermodynamic parameters for adsorption of chromium(VI) onto hal-HDTMA.

Table 4
Thermodynamic parameters and isosteric heat of chromium(VI) adsorption on HDTMA modified halloysite

Thermodynamic parameters			
Temperature (K)	ΔG (kJ/mol)	ΔH (kJ/mol)	ΔS (J/mol K)
293	–18.46	–21.28	–9.34
303	–18.65		
313	–18.34		
323	–18.20		
Isosteric heat of adsorption			
q_e (mg/g)	ΔH_x (kJ/mol)		R^2
0.6	–20.21		0.9882
1.0	–19.84		0.9908
1.2	–19.16		0.9903

3.2.6. Isosteric adsorption heat

Isosteric adsorption heat (ΔH_x, [kJ/mol]) is the adsorption process heat at constant coverage of the adsorbent surface.

The value of isosteric adsorption heat is calculated on the basis of the Clausius–Clapeyron equation:

$$\left(\frac{d \ln C_e}{dT}\right)_Q = -\frac{\Delta H_x}{RT^2} \tag{19}$$

Its linear relationship is illustrated in the following formula:

$$\ln C_e = \frac{\Delta H_x}{R} \times \frac{1}{T} + \text{const} \tag{20}$$

Direction coefficient of the straight line ln C_e versus 1/T corresponds to $\frac{\Delta H_x}{R}$.

The diagram of the aforementioned relationship for adsorbing surface coverage, that is, 1.2, 1.0, as well as 0.6 mg/g, is given in Figs. 10(a)–(c), respectively.

The values of ΔH_x are shown in Table 4. The determined ΔH_x values are negative, ca. –20 kJ/mol, which confirms the exothermic character of the chromium(VI) adsorption process on the modified halloysite adsorbent. ΔH_x value <80 kJ/mol proves the physical character of adsorption in the discussed arrays.

3.2.7. Efficiency of removing chromium(VI)

The effectiveness of the toxic contamination removal process is vital with respect to a range of various concentration levels of compounds in the solution.

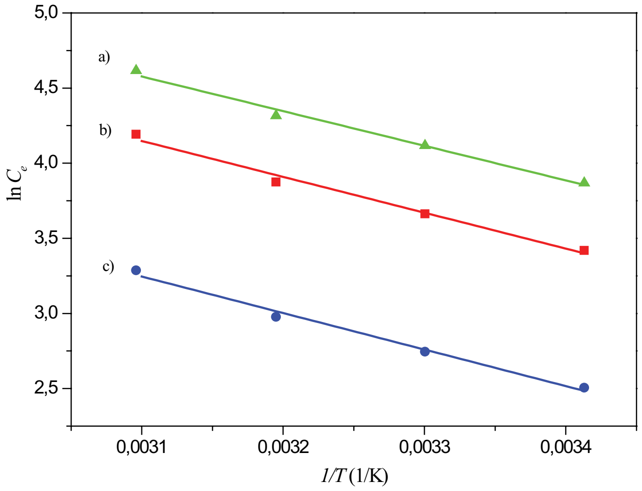

Fig. 10. Plot of lnC_e against 1/T for the adsorption of chromium(VI) onto hal-HDMTA (surface coverage is: (a) 1.2 mg/g, (b) 1.0 mg/g, (c) 0.6 mg/g).

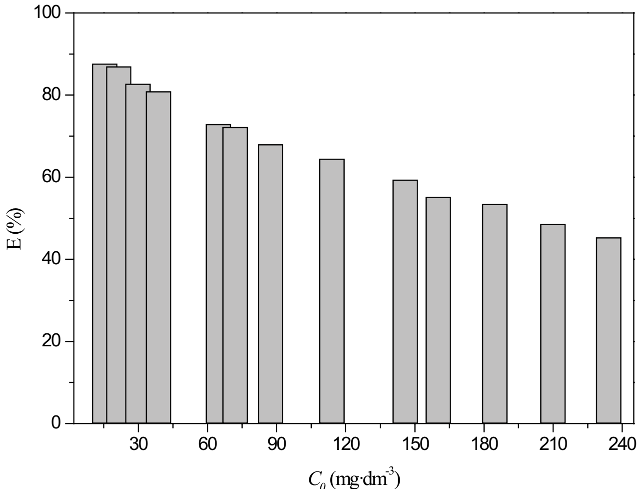

Fig. 11. The efficiency of the chromium(VI) removal from aqueous solution by HDTMA-modified halloysite.

The results of studies on the dependence between sorption efficiency and initial concentration of chromium(VI) in the solution, Fig. 11, show that at concentrations up to ca. 40 mg/dm^3, the process efficiency exceeds 80%. At higher concentration values, sorption gradually decreases. At the content level of 230 mg/dm^3, the efficiency is still relatively high and is over 45%. The efficiency of removing toxic chromium(VI) from the solution with the use of modified halloysite, particularly at its low concentration levels, is utterly satisfactory.

4. Conclusion

The results of research show that HDTMA is an efficient modifying compound, which changes halloysite surface charge from negative to positive. Modified halloysite can be successfully used as an anion sorbent. As a result of this modification, the hexadecyltrimethylammonium cations are bonded to clay mineral surface without any distortions of halloysite structure. Completed comparative analysis of spectra in infrared for raw halloysite and hal-HDTMA indicates that, depending on surfactant concentration in the solution, modified halloysite surface may be covered with the HDTMA$^+$ cations in the form of a monolayer, bilayer, or hemi-micelle. Both bilayer and micellar covering of the adsorbent surface make adsorption of anionic forms possible.

The studies on chromium(VI) anions adsorption on the modified halloysite have proven that the process is most efficient from acidic solutions, at pH ranging from 2.1 to 6. In these conditions, the solution contains dichromate $Cr_2O_7^{2-}$ and hydrogenchromate $HCrO_4^-$ ions in equilibrium. It can be assumed that chromium(VI) adsorption on halloysite modified using the HDTMA$^+$ cations proceeds through the interaction of both $Cr_2O_7^{2-}$ and $HCrO_4^-$ anions with a positive charge of the ammonium part of the molecule, the so-called surfactant "head."

Sorption of chromium(VI) anions on modified halloysite takes place according to the kinetics of pseudo-second-order. It has been observed that neither intraparticle diffusion nor "diffusion by film" is the stage that decides about the rate of the whole process.

Isotherms of the chromium(VI) sorption on the modified sorbent hal-HDTMA correlate best with the theoretical model described by the Langmuir isotherm. Adsorption of the Cr(VI) anions has the nature of a physical process, which is indicated by the determined activation energy value of 7.603 kJ/mol and the enthalpy ΔH of –22.29 kJ/mol. Negative values of enthalpy and (ΔH) and isosteric adsorption heat (ΔH_x) point out exothermic nature of the analysed process.

Sorption of the Cr(VI) from solutions with concentrations up to 40 mg/dm^3 proceeds with efficiency exceeding 80%. This shows the potential of using halloysite modified with HDTMA to purify sewage with low anion concentration level. At high chromium(VI) concentration values sorption output gradually decreases, but even at ca. 230 mg/dm^3 the process efficiency is still high, reaching ca. 45%.

References

[1] V.K. Gupta, I. Ali, T.A. Saleh, A. Nayak, S. Agarwal, Chemical treatment technologies for waste-water recycling – an overview, RSC Adv., 2 (2012) 6380–6388.

[2] K. Ait Bentaleb, E. El Khattabi, M. Lakraimi, L. Benaziz, E. Sabbar, M. Berraho, A. Legrouri, Removal of Cr(VI) from wastewater by anionic clays, J. Mater. Environ. Sci., 7 (2016) 2886–2896.

[3] J. Lach, E. Ociepa, Effect of the process of Wg-12 activated carbon modification on the sorption of chromium, Ecol. Chem. Eng. A, 20 (2013) 731–739.

[4] J. Acharya, J.N. Sahu, B.K. Sahoo, C.R. Mohanty, B.C. Meikap, Removal of chromium(VI) from wastewater by activated carbon developed from Tamarind wood activated with zinc chloride, Chem. Eng. J., 150 (2009) 25–39.

[5] D. Mohan, K.P. Singh, V.K. Singh, Removal of hexavalent chromium from aqueous solution using low-cost activated carbons derived from agricultural waste materials and activated carbon fabric cloth, Ind. Eng. Chem. Res., 44 (2005) 1027–1042.

[6] A. Türkan, Y. Kar, Removal of Cr(VI) from aqueous solution by pyrolytic charcoals, New Carbon Mater., 31 (2016) 501–509.

[7] G. Tiravanti, D. Petruzzelli, R. Passino, Pretreatment of tannery wastewaters by an ion exchange process for Cr(III) removal and recovery, Water Sci. Technol., 36 (1997) 197–207.

[8] C. Balan, I. Volf, D. Bilba, Chromium (VI) Removal from aqueous solutions by purolite base anion-exchange resins with gel structure, Chem. Ind. Chem. Eng. Q, 19 (2013) 615–628.

[9] C.A. Kozlowski, W. Walkowiak, Removal of chromium(VI) from aqueous solutions by polymer inclusion membranes, Water Res., 36 (2002) 4870–4876.

[10] T.Zh. Sadyrbaeva, Removal of chromium(VI) from aqueous solutions using a novel hybrid liquid membrane-electrodialysis process, Chem. Eng. Process., 99 (2016) 183–191.

[11] N. Kongsricharoern, C. Polprasert, Chromium removal by a bipolar electrochemical precipitation process, Water Sci. Technol., 34 (1996) 109–116.

[12] A.R. Rahmani, E. Hossieni, A. Poormohammadi, Removal of chromium (VI) from aqueous solution using electro-Fenton process, Environ. Process., 2 (2015) 419–428.

[13] Z. Li, R. Bowman, Retention of inorganic oxyanions by organo-kaolinite, Water Res., 35 (2001) 3771–3776.

[14] M. Majdan, S. Pikus, Z. Rzączyńska, M. Iwan, O. Maryuk, R. Kwiatkowski, H. Skrzypek, Characteristics of chabazite modified by hexadecyltrimethylammonium bromide and of its affinity toward chromates, J. Mol. Struct., 791 (2006) 53–60.

[15] M. Majdan, O. Maryuk, S. Pikus, E. Olszewska, R. Kwiatkowski, H. Skrzypek, Equilibrium, FTIR, scanning electron microscopy and small wide angle X-ray scattering studies of chromates adsorption on modified bentonite, J. Mol. Struct., 740 (2005) 203–211.

[16] Z. Li, R.S. Bowman, Counterion effects on the sorption of cationic surfactant and chromate on natural clinoptilolite, Environ. Sci. Technol., 31 (1997) 2407–2412.

[17] B.S. Krishna, D.S.R. Murty, B.S. Jai Prakash, Surfactant-modified clay as adsorbent for chromate, Appl. Clay Sci., 20 (2001) 65–71.

[18] R. Eisler, Chromium hazards to fish, wildlife, and invertebrates: a synoptic review, U.S. Fish Wildl. Serv. Biol. Rep., 85 (1986) 1–38.

[19] C.B. Vidal, G.S. Raulino, A.L. Barros, A.C. Lima, J.P. Ribeiro, M.J. Pires, R.F. Nascimento, Equilibrium isotherm studies for the sorption of benzene, toluene, and phenol onto organo-zeolites and as-synthesized MCM-41M, Sep. Purif. Technol., 40 (2004) 217–229.

[20] J.E. Gieseking, The mechanism of cation exchange in the montmorillonitebeidellite-nontronite type of clay minerals, Soil Sci., 47 (1939) 1–14.

[21] S.M. Lee, D. Tiwari, Organo and inorgano-organo-modified clays in the remediation of aqueous solutions: an overview, Appl. Clay Sci., 59–60 (2012) 84–102.

[22] L.B. de Paiva, A.R. Moralesa, F.R. Valenzuela Diaz, Organoclays: properties, preparation and applications, Appl. Clay Sci., 42 (2008) 8–24.

[23] G.M. Haggerty, R.S. Bowman, Sorption of chromate and other inorganic anions by organo-zeolite, Environ. Sci. Technol., 28 (1994) 452–458.

[24] H. Guan, E. Bestland, C. Zhu, H. Zhu, D. Albertsdottir, J. Hutson, C.T. Simmons, M. Ginic-Markovic, X. Tao, A.V. Ellis, Variation in performance of surfactant loading and resulting nitrate removal among four selected natural zeolites, J. Hazard. Mater., 183 (2010) 616–621.

[25] J. Schick, P. Caullet, J.L. Paillaud, J. Patarin, C. Mangold-Callarec, Batchwise nitrate removal from water on a surfactant-modified zeolite, Microporous Mesoporous Mater., 132 (2010) 395–400.

[26] Z. Li, L. Gallus, Surface configuration of sorbed hexadecyltrimethylammonium on kaolinite as indicated by surfactant and counterion sorption, cation desorption, and FTIR, Colloids Surf. A: Physicochem. Eng. Aspects, 264 (2005) 61–67.

[27] ASTM (American Society for Testing And Materials), Standard Methods for the Examination of Water and Wastewater, 18th ed., American Public Health Association, Washington, 1992.

[28] K.S.W. Sing, D.H. Everett, R.A.W. Haul, L. Moscou, R.A. Pierotti, J. Rouquerol, T. Siemianowska, Reporting physisorption data for gas/solid systems with special reference to the determination of surface area and porosity, Pure Appl. Chem., 57 (1985) 603–619.

[29] S. Brunauer, P.H. Emett, E. Teller, Adsorption of gases in multimolecular layers, J. Am. Chem. Soc., 60 (1938) 309–319.

[30] R.L. Frost, J. Yang, H. Cheng, A spectroscopic comparison of selected Chinese kaolinite, coal bearing kaolinite and halloysite: a midinfrared and near infrared study, Spectrochim. Acta A: Mol. Biomol. Spectrosc., 77 (2010) 856–861.

[31] Z. Li, W.T. Jiang, H. Hong, An FTIR investigation of hexadecyltrimethylammonium intercalation into rectorite, Spectrochim. Acta A: Mol. Biomol. Spectrosc., 71 (2008) 1525–1534.

[32] J. Madejova, H. Palkova, P. Kamadel, IR Spectroscopy of Clay Minerals and Clay Nanocomposites, J. Yarwood, R. Douthwaite, S. Duckett, Eds., Spectroscopic Properties of Inorganic and Organometallic Compounds: Techniques, Materials and Applications, Royal Society of Chemistry, Cambridge, UK, Vol. 41, 2010, pp. 22–71.

[33] Y. Xi, Z. Ding, H. He, R.L. Frost, Infrared spectroscopy of organoclays synthesized with the surfactant octadecyltrimethylammonium bromide, Spectrochim. Acta A: Mol. Biomol. Spectrosc., 61 (2005) 515–525.

[34] M. Majdan, O. Maryuk, A. Gładysz-Płaska, S. Pikusa, R. Kwiatkowski, Spectral characteristics of the bentonite loaded with benzyldimethyloctadecylammonium chloride, hexadecyltrimethylammonium bromide and dimethyldioctadecylammonium bromide, J. Mol. Struct., 874 (2008) 101–107.

[35] H.P. He, R.L. Frost, T. Bostrom, P. Yuan, L. Duong, D. Yang, X.F. Xi, T.J. Kloprogge, Changes in the morphology of organoclays with HDTMA+ surfactant loading, Appl. Clay Sci., 31 (2006) 262–271.

[36] E.J. Sullivan, D.B. Hunter, R.S. Bowman, Topological and thermal properties of surfactant-modified clinoptilolite studied by Tapping-mode atomic force microscopy and high-resolution thermogravimetric analysis, Clays Clay Miner., 45 (1997) 42–53.

[37] E.J. Sullivan, D.B. Hunter, R.S. Bowman, Fourier transform Raman spectroscopy of sorbed HDTMA and the mechanism of chromate sorption to surfactant-modified clinoptilolite, Environ. Sci. Technol., 32 (1998) 1948–1995.

[38] D. Palmer, R.W. Puls, Natural Attenuation of Hexavalent Chromium in Groundwater and Soils, EPA/540/5-94/505. U.S. EPA, Office of Solid Waste and Emergency Response and Office of Research and Development, Ada, Oklahoma, 1994.

[39] D.L. Sparks, Kinetics of Reaction in Pure and Mixed Systems, Soil Physical Chemistry, CRC Press, Boca Raton, Florida, 1986.

[40] R.S. Juang, M.L. Chen, Application of the Elovich equation to the kinetics of metal sorption with solvent-impregnated resins, Ind. Eng. Chem. Res., 36 (1997) 813–820.

[41] S. Lagergren, About the theory of so called adsorption of soluble substances, K. Sven. Vetensk. Akad. Handl., 24 (1898) 1–39.

[42] G. Blachard, M. Maunayer, G. Martin, Removal of heavy metals from waters by means of natural zeolites, Water Res., 18 (1984) 1501–1507.

[43] Y.S. Ho, D.A.J. Wase, C.F. Forster, Kinetic studies of competitive heavy metal adsorption by sphagnum moss peat, Environ. Technol., 17 (1996) 71–77.

[44] Y.S. Ho, G. McKay, Pseudo-second order model for sorption processes, Process Biochem., 34 (1999) 451–465.

[45] W.J. Weber, J.C. Morris, Kinetics of adsorption of carbon from solution, J. Sanit. Eng. Div. Am. Soc. Civ. Eng., 89 (1963) 31–60.

[46] T.S. Anirudhan, P.G. Radhakrishnan, Thermodynamics and kinetics of adsorption of Cu(II) from aqueous solutions onto a new cation exchanger derived from tamarind fruit shell, J. Chem. Thermodyn., 40 (2008) 702–709.

[47] G.E. Boyd, A.W. Adamson, L.S. Meyers, The exchange adsorption of ions from aqueous solution by organic zeolites. II, Kinetics, J. Am. Chem. Soc., 69 (1947) 2836–2848.

[48] D. Reichenberg, Properties of ion exchange resins in relation to their structure. III. Kinetics of exchange, J. Am. Chem. Soc., 75 (1953) 589–597.

[49] M.J. Temkin, V. Pyzhev, Recent modifications to Langmuir isotherms, Acta Phys. Chim. USSR, 12 (1940) 327–356.

[50] M.M. Dubinin, L.V. Radushkevich, The equation of the characteristic curve of activated charcoal, Proc. Acad. Sci. USSR, 55 (1947) 331–337.

[51] M.M. Dubinin, The potential theory of adsorption of gasses and vapors for adsorbents with energetically nonuniform surfaces, Chem. Rev., 60 (1960) 235–266.

[52] H.M.F. Freundlich, Over the adsorption in solution, J. Phys. Chem., 57 (1906) 385–470.

[53] I. Langmuir, The constitution and fundamental properties of solids and liquids. Part I. Solids, J. Am. Chem. Soc., 38 (1916) 2221–2295.

[54] S.M. Hasany, M.H. Chaudhary, Sorption potential of Hare River sand for the removal of antimony from acidic aqueous solution, Appl. Radiat. Isot., 47 (1996) 467–471.

[55] Q. Li, L. Chai, Z. Yang, Q. Wang, Kinetics and thermodynamics of Pb(II) adsorption onto modified spent grain from aqueous solutions, Appl. Surf. Sci., 255 (2009) 4298–4303.

[56] C.H. Giles, D. Smith, A. Huitson, A general treatment and classification of the solute adsorption isotherm, I. Theoretical, J. Colloid Interface Sci., 47 (1974) 755–765.